analytical chemistry

pubs.acs.org/ac Article

A Catalyst Tube-Equipped Dual-Stage Tube Furnace System for Accurate Hg Isotopic Determination of Ore Samples Using Neptune Plus Multicollector Inductively Coupled Plasma Mass Spectrometry

Lingjian Gao, Deyou Sun, Xueyun Wang, Di Chen, Zhendong Tian, Anbo Luo, and Runsheng Yin*

Cite This: *Anal. Chem.* 2024, 96, 17560−17566 Read Online

ACCESS | Metrics & More | Article Recommendations | Supporting Information

ABSTRACT: Mercury (Hg) isotopes, which display mass-dependent fractionation and mass-independent fractionation, provide a multidimensional tracer to decipher the source of metals in mineral deposits. However, mineral ore samples usually contain abundant interfering elements (e.g., Te) that can cause inaccurate Hg isotopic analysis. Available acid digestion and combustion methods failed to remove these interfering elements, hindering the application of Hg isotopes for metallogenetic tracing. Here, we developed a new dual-stage tube furnace system employing a Mn-containing catalyst tube to pretreat mineral ore samples. This method yielded good Hg recoveries (100.5 ± 3.8%, 1SD, n = 15) and low levels of interfering elements in sample solutions, allowing for accurate analysis of a series of ore standard reference materials (GBW-11108v: coal; GSO-3: Cu−Ag sulfide ore; GBW 07859: Au−Te sulfide ore). The new method was also successfully applied to measure the Hg isotopic composition of magmatic and hydrothermal ore deposits, which yielded a large range in Δ^{199}Hg value (−0.19 to 0.22‰) for ore deposits formed in different geological settings, highlighting the future applications of this method for metallogenic tracing, especially tracing the source of metals in mineral ore deposits.

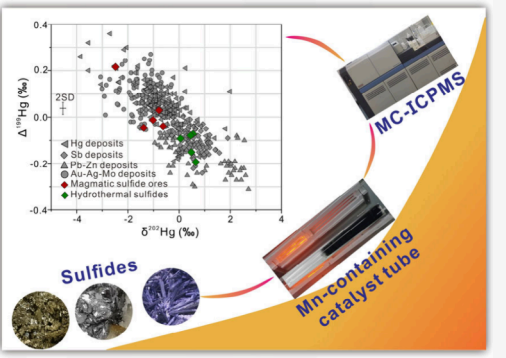

INTRODUCTION

Mercury (Hg) is a redox-sensitive, volatile, and toxic metal,[1] whose stable isotopes (196, 198−202, 204 amu) undergo mass-dependent fractionation (MDF, typically reported as δ^{202}Hg) and mass-independent fractionation (MIF, typically reported as Δ^{199}Hg).[2] Hg-MDF occurs ubiquitously during physical, chemical and biological processes, whereas Hg-MIF occurs mainly during photochemical processes (e.g., photoreduction of Hg(II) and photodegradation of methylmercury).[3] Large variations of >10‰ for both δ^{202}Hg and Δ^{199}Hg have been observed in different environmental pools, providing two-dimensional information on the sources and fates of Hg in the environment.[3−5] Multicollector inductively coupled plasma mass spectrometry (MC-ICP-MS), combined with an online Hg(0) introduction system enabling complete reduction of Hg(II) by Tin(II) chloride ($SnCl_2$) to gaseous Hg(0), has been employed to determine the isotopic composition of Hg.[2,6−8] Prior to Hg isotopic analyses, acid digestion or combustion methods are usually applied to transfer Hg from sample powders into sample solutions, with good Hg recoveries (90 to 110%), sufficiently high Hg concentrations (0.3−0.5 ng/mL) and proper acid levels (5 to 20%, v/v).[8,9]

The acid digestion method is useful for preparing samples containing Hg > 15 ng/g, such as sediments and soil. For these samples, typically ∼0.2 g of sample powder is digested in 5 mL of aqua regia (HNO_3/HCl = 1/3, v/v), which can yield good recoveries and solutions with suitable Hg concentrations and acid content for MC-ICP-MS analysis.[9−14] However, the acid digestion method fails to prepare samples with low Hg abundance (<15 ng/g; e.g., igneous rocks) and high organic matter content (e.g., coal and black shale). The combustion method, involving a dual-stage tube furnace to thermally release all Hg species from samples into highly oxidized trapping solutions containing 40% reverse aqua regia (HNO_3/HCl = 2/1, v/v) or 1% $KMnO_4$, was developed for preparing low-Hg and high-organic samples.[15−18] The combustion method can prepare a large mass of samples, resulting in suitable Hg and acid concentrations in the sample solutions. However, certain types of ore samples (e.g., magmatic and hydrothermal sulfides) contain abundant interfering elements (e.g., Te), which are volatile and readily transferred into trapping solutions using available acid digestion and combustion methods. These interfering elements can cause an incomplete reduction of Hg(II) by $SnCl_2$ during Hg isotope analysis, resulting in false Hg isotopic ratios. To ensure the

Received: June 13, 2024
Revised: October 15, 2024
Accepted: October 15, 2024
Published: October 24, 2024

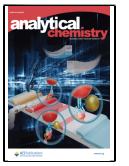

https://doi.org/10.1021/acs.analchem.4c03041
Anal. Chem. 2024, 96, 17560−17566

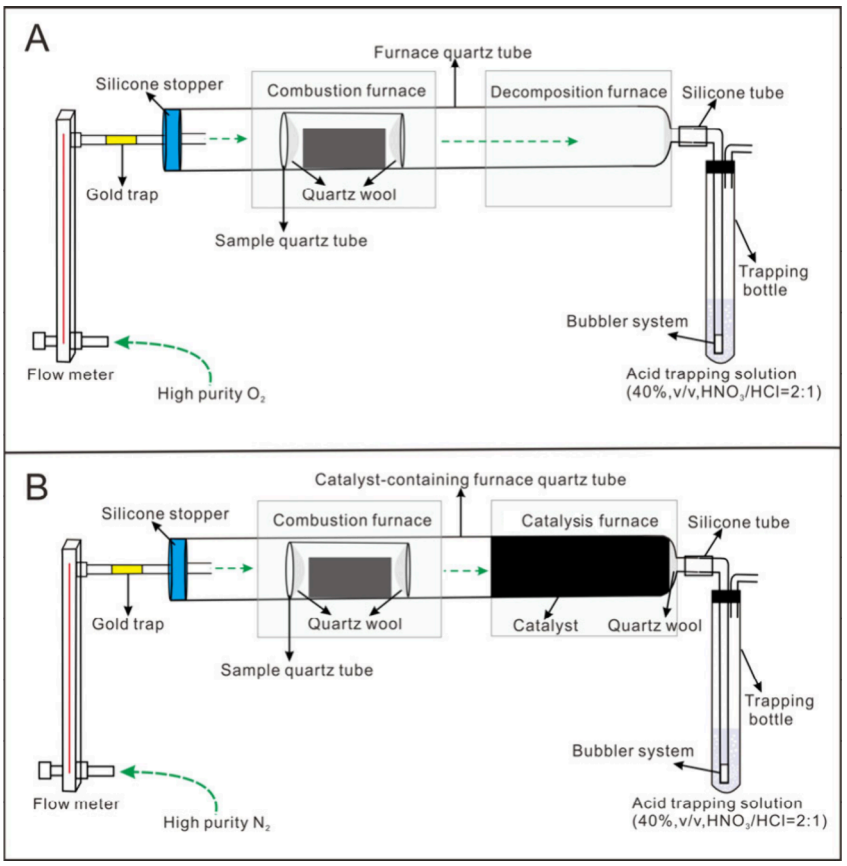

Figure 1. Schematic diagram of the dual-stage tube system. (A) The dual-stage tube furnace system with the conventional tube; (B) The dual-stage tube furnace system with the newly developed catalyst tube.

accurate analysis of ore samples, modification of the available double-stage tube furnace system to remove volatile inferencing elements is warranted.

In this work, we developed a new dual-stage tube furnace system employing a Mn-containing catalyst tube to prepare ore samples containing abundant interfering elements. Regarding a series of mineral ore standard reference materials (SRMs) and mineral ore samples from different types of mineral deposits, our new method gained better Hg recoveries in sample solutions than traditional acid digestion and combustion methods. We demonstrate that interfering elements can be effectively captured by the Mn-containing catalyst tube, which allows for the accurate determination of the Hg isotopic composition of ore deposits.

EXPERIMENTAL METHODS

Materials and Reagents. The catalyst tube (W/PACKING 614−822−105), consisting of manganese dioxide, cobalt oxide, and calcium oxide, was purchased from LECO Corporation, USA. GBW-11108v (coal), GSO-3 (Cu−Ag sulfide ore), and GBW 07859 (Au−Te sulfide ore) were ore SRMs used to assess the accuracy of our method. Sulfide ore samples from the Jinchuan magmatic Ni−Cu sulfide deposit (n = 5),[19] the Pulang porphyry Cu−Au deposit (n = 3)[20] and the Zhibula skarn Cu polymetallic deposit (n = 1)[21] in China were used to access the validity of our method. These samples were cleaned with 18.2 MΩ cm water, air-dried, powdered, and homogenized prior to use.

18.2 MΩ·cm water and ultrapure grade acids (HCl and HNO_3) were used for preparing all the solutions. Aqua regia (HCl/HNO_3 = 3/1, v/v) were made for sample digestion. Reverse aqua regia (HNO_3/HCl = 2/1, v/v, in 40% v/v) was prepared as trapping solutions for preparing samples using the dual-stage tube furnace system. The solution containing 3% $SnCl_2$ (w/v) in 10% HCl (v/v) was prepared as a reductant of Hg(II) in sample solutions during Hg concentration and isotopic composition analyses. National Institute of Standards and Technology (NIST) SRM 3133 and NIST SRM 3177 Hg standard solutions both containing 1 ng/mL Hg in 10% HCl (v/v) and NIST SRM 997 Tl standard solutions containing 25 ng/mL Tl in 3% HNO_3 (v/v) were prepared for Hg isotope analysis. The 3% HNO_3 (v/v) washing solution was used for Hg isotope analysis.

Sample Preparation. The SRMs and sulfide ore samples were prepared using three methods: (1) acid digestion, (2) the dual-stage tube furnace employing a traditional furnace quartz tube (Figure 1A), and (3) the dual-stage tube furnace employing a catalyst-containing furnace quartz tube (Figure 1B).

Regarding the acid digestion method, ∼0.2 g of mineral ore SRMs and sulfide ore samples were digested with 5 mL of aqua regia at 95 °C for 3 h in a water bath.[9,12] The solutions were diluted to acid concentrations of <20% prior to trace element concentrations, Hg concentration, and Hg isotopic composition analyses.

Regarding the combustion method, ∼0.05 to 5 g of SRMs and sulfide ore samples were prepared using the traditional dual-stage tube furnace system (Figure 1A) and the new dual-stage tube furnace system (Figure 1B). Both systems used quartz tubes with the same size (OD: 26 mm; ID: 22 mm;

https://doi.org/10.1021/acs.analchem.4c03041
Anal. Chem. 2024, 96, 17560−17566

Length: 0.9 m). The former used O_2 as the carrier gas, and the latter used N_2 as the carrier gas. For both systems, a dynamic temperature programming of the first furnace, with a temperature ramp from ambient temperature to 950 °C in 40 min (i.e., 23−24 degrees per minute) and holding 950 °C in 50 min, was used to efficiently release Hg from the samples, given that all Hg compounds (e.g., $HgCl_2$, HgS, $HgSO_4$ and HgO) would transform to gaseous Hg(0) under 700 °C.[22] The second furnace kept a constant temperature at 700 °C to ensure that released Hg was not adsorbed on the wall of the quartz tubes. During each run, weighed sample powders were loaded into a sample boat which is a quartz tube (OD: 20 mm; ID: 18 mm; Length: 10 cm) and capped with quartz wool (precleaned at 480 °C for 1.5 h) at both ends to avoid particle release during combustion. A gold trap was equipped to the gas line of the N_2 gas bottle, producing Hg-free carrier gas (O_2 or N_2) that was introduced to the dual-stage tube furnace system at a constant flow rate (25 mL/min) to flush the product Hg(0) into the trapping solution (5 mL of 40% reverse aqua regia, v/v). The acid trapping device comprises a 25 mL borosilicate glass bubble bottle and an elbow-shaped custom-made fritted glass tube. After a combustion-trapping procedure, the trapping solution was transferred into a 40 mL lucifugal borosilicate glass bottle (precleaned at 480 °C in a muffle furnace for 1.5 h) at 4 °C prior to trace element concentration, Hg concentration, and Hg isotopic composition analyses.

Analyses of Trace Element Concentrations. The sample solutions yielded from the three pretreatment methods were subjected to trace element concentration analyses using Agilent 8900 inductively coupled plasma mass spectrometry at the Institute of Geochemistry, Chinese Academy of Sciences (IGCAS). The analyzed elements included V, Cr, Co, Ni, Mo, Th, U, rare earth elements (La, Ce, Pr, Nd, Sm, Eu, Gd, Dy, Ho, Er, Tm, Y and Yb), Ba, Mn, Cu, Ag, Sb As, Zn, Tl, Pb, Cd, and Te. Agilent 5183−4688 and 8500−6944 multielement standard solutions were analyzed every 10 samples, yielding recoveries of 92 to 97% and uncertainties of <5% (2SD) for the analyzed elements.

Analyses of Hg Concentration and Isotopic Composition. The total Hg (THg) concentrations of SRMs and sulfide ore samples were directly measured using Milestone DMA-80 Hg analyzer at IGCAS. The Hg detection limit was lower than 0.01 ppb. Analysis of soil standard reference materials GSS-4 (n = 3) and GBW 07859 (n = 3) yielded Hg recoveries of 90 to 110% and uncertainties of <10% (2SD). For comparison, the solutions yielded from the three pretreatment methods were subjected to THg concentration analyses using F732−S cold vapor atomic absorption spectrometry at IGCAS. Analysis of the Hg isotopic composition was done using Neptune Plus multicollector inductively coupled plasma mass spectrometry.[8] Before analysis, the sample solutions were diluted to 1 ng/mL Hg in 10 to 20% (v/v) reverse aqua regia (HNO_3/HCl = 2/1, v/v) using 18.2 MΩ·cm water. Instrumental mass bias was corrected using NIST SRM 997 Tl standard solution (25 ng/mL Tl in 3% HNO_3 (v/v)) introduced by an Aridus II desolvating nebulizer. The Hg isotopic composition was reported following the convention recommended by Bergquist and Blum.[2] Hg-MDF is expressed in δ^{xxx}Hg notation in units of permil (‰) referenced to the NIST-3133 Hg standard (analyzed before and after each sample):

$$\Delta^{xxx}\mathrm{Hg}(‰) = [(^{xxx}\mathrm{Hg}/^{198}\mathrm{Hg}_{sample})/(^{xxx}\mathrm{Hg}/^{198}\mathrm{Hg}_{standard}) - 1] \times 1000 \quad (1)$$

where xxx refers to 199, 200, 201, and 202. Hg-MIF is reported in Δ notation, which describes the difference between the measured δ^{xxx}Hg and the theoretically predicted δ^{xxx}Hg value, in units of permil (‰):

$$\Delta^{xxx}\mathrm{Hg} \approx \delta^{xxx}\mathrm{Hg} - \delta^{202}\mathrm{Hg} \times \beta \quad (2)$$

β is equal to 0.2520 for ^{199}Hg, 0.5024 for ^{200}Hg, and 0.7520 for ^{201}Hg, respectively. NIST-3177 secondary standard solutions were measured every 10 samples. The overall average and uncertainty of NIST-3177 (δ^{202}Hg: −0.53 ± 0.10‰; Δ^{199}Hg: 0.01 ± 0.05‰; Δ^{200}Hg: 0.02 ± 0.05‰; Δ^{201}Hg: 0.04 ± 0.06‰; 2SD, n= 4) and GSS-4 (δ^{202}Hg: −1.64 ± 0.10‰; Δ^{199}Hg: −0.47 ± 0.03‰; Δ^{200}Hg: −0.02 ± 0.06‰; Δ^{201}Hg: −0.40 ± 0.05‰; 2SD, n= 4) agree well with previous results.[2,18,23] The largest values of standard deviations (2SD) for NIST-3177 and GSS-4 were used to reflect analytical uncertainties.

RESULTS AND DISCUSSION

Hg Recoveries of Different Pretreatment Methods. The analytical results of THg are given in Supplementary Table S1. The THg concentrations of SRMs GBW-11108v, GSO-3 and GBW 07859, measured by the DMA-80 Hg analyzer, are 154 ± 5 ppb (n = 3, 1SD), 295 ± 3 ppb (n = 3, 1SD) and 642 ± 9 (n = 3, 1SD), respectively, consistent with certified values. The THg concentrations of magmatic and hydrothermal sulfide samples, measured by the DMA-80 Hg analyzer, range from 3.54 to 124 ppb and from 57 to 609 ppb, respectively (Table S1). Below, the results analyzed by the DMA-80 Hg analyzer were compared with the Hg concentrations (Tables S2−3) based on analyses of sample solutions to assess the Hg recoveries of the three pretreatment methods.

Regarding SRMs GBW-11108v, GSO-3 and GBW 07859, analysis of digestion solutions yielded THg concentrations of 111 ± 4.4 ppb (n = 3, 1SD), 300 ± 5.2 ppb, and 661 ± 8.2 ppb (n = 3, 1SD), with THg recoveries of 72 ± 2.8% (n = 3, 1SD), 101 ± 1.9% (n = 3, 1SD) and 103 ± 1.3% (n = 3, 1SD), respectively (Table S2). Analysis of sample solutions pretreated by the dual-stage tube furnace with the traditional furnace quartz tube yielded THg concentrations of 160 ± 4.7 ppb (n = 3, 1SD), 275 ± 17 ppb (n = 3, 1SD) and 636 ± 27 ppb (n = 3, 1SD) for GBW-11108v, GSO-3 and GBW 07859, with THg recoveries of 104 ± 3.0% (n = 3, 1SD), 92 ± 5.6% (n = 3, 1SD) and 99 ± 3.5% (n = 3, 1SD), respectively. Analysis of sample solutions pretreated by the dual-stage tube furnace with the catalyst-containing furnace quartz tube yielded THg concentrations of 152 ± 4.8 ppb (n = 6, 1SD), 296 ± 7.4 ppb (n = 6, 1SD) and 654 ± 27 ppb (n = 6, 1SD), with THg recoveries of 99 ± 3.2% (n = 6, 1SD), 100 ± 2.5% (n = 6, 1SD) and 102 ± 4.3% (n = 6, 1SD), respectively.

Regarding sulfide samples, analysis of digestion solutions yielded THg concentrations ranging from 0 to 489 ppb with THg recoveries of 0 to 80.2%. Analysis of sample solutions pretreated by the dual-stage tube furnace with a traditional furnace quartz tube yielded THg concentrations of 2.9 to 116 ppb with THg recoveries of 0 to 50.4%. Analysis of sample solutions pretreated by the dual-stage tube furnace with the catalyst-containing furnace quartz tube yielded THg concen-

https://doi.org/10.1021/acs.analchem.4c03041
Anal. Chem. 2024, 96, 17560−17566

trations of 3.3 to 569 ppb with THg recoveries of 93 to 103% (Supplementary Table S3).

The results from our new method yielded better THg recoveries than the other two traditional methods (Figure 2),

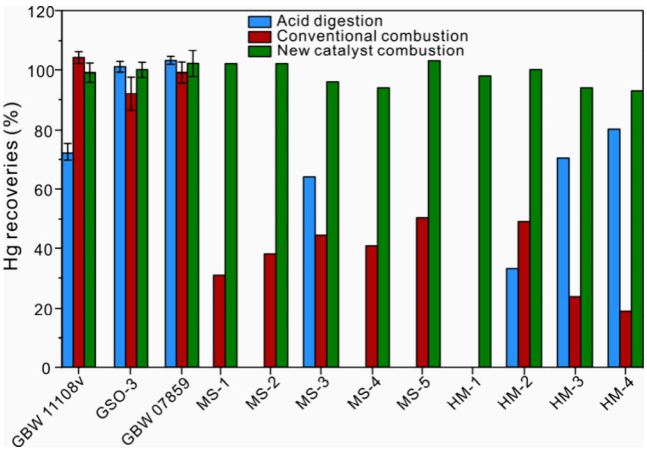

Figure 2. Hg recoveries of GBW 11108v, GSO-3, GBW 07859, magmatic sulfide ores and hydrothermal sulfides prepared using acid digestion method, conventional combustion and new catalyst combustion.

both of which may introduce interfering elements in sample solutions and result in a decrease in reduction efficiency of Hg(II) by $SnCl_2$ during THg concentration analysis using F732−S cold vapor atomic absorption spectrometry.

Hg Isotopic Composition of SRMs. The Hg isotopic composition of SRMs based on the three pretreatment methods is shown in Supplementary Table S2. Since our new method yielded recoveries of ∼100% for sample solutions of all SRMs, the Hg isotopic results of our new method can reflect the real Hg isotopic composition; i.e., GBW-11108v displays δ^{202}Hg and Δ^{199}Hg values of −1.02 ± 0.05 ‰ and −0.31 ± 0.03‰ (n = 6, 1SD), respectively; GSO-3 displays δ^{202}Hg and Δ^{199}Hg values of 0.25 ± 0.04 ‰ and −0.12 ± 0.02‰ (n = 6, 1SD), respectively; and GBW 07859 displays δ^{202}Hg and Δ^{199}Hg values of −0.97 ± 0.06 ‰ and 0.08 ± 0.03 ‰ (n = 6, 1SD), respectively.

Measurements of digested samples yielded δ^{202}Hg and Δ^{199}Hg values of −1.14 ± 0.20‰ and −0.17 ± 0.01‰ (n = 3, 1SD) respectively for GBW-11108v; 0.29 ± 0.21‰ and −0.07 ± 0.02‰ (n = 3, 1SD) respectively for GSO-3; and −0.06 ± 0.05‰ and −0.00 ± 0.04‰ (n = 3, 1SD) respectively for GBW 07859. Measurements of sample solutions pretreated by the dual-stage tube furnace with a traditional furnace quartz tube yielded δ^{202}Hg and Δ^{199}Hg values of −1.03 ± 0.11‰ and −0.31 ± 0.02‰ (n = 3, 1SD) respectively for GBW-11108v, 0.11 ± 0.43‰ and −0.03 ± 0.04‰ (n = 3, 1SD) respectively for GSO-3, and −0.22 ± 0.23‰ and 0.00 ± 0.06‰ (n = 3, 1SD) respectively for GBW 07859. As shown in Figure 3, compared with the results from our new method, GSO-3 and GBW 07859 pretreated by the two traditional methods display either positive or negative shifts in δ^{202}Hg and Δ^{199}Hg values, although they had good recoveries. The sample solutions yielded from the two traditional methods may contain interfering elements that can influence Hg isotopic ratios, as discussed below.

Interfering Elements during Hg Isotopic Analyses. Potential interfering elements in the samples include refractory

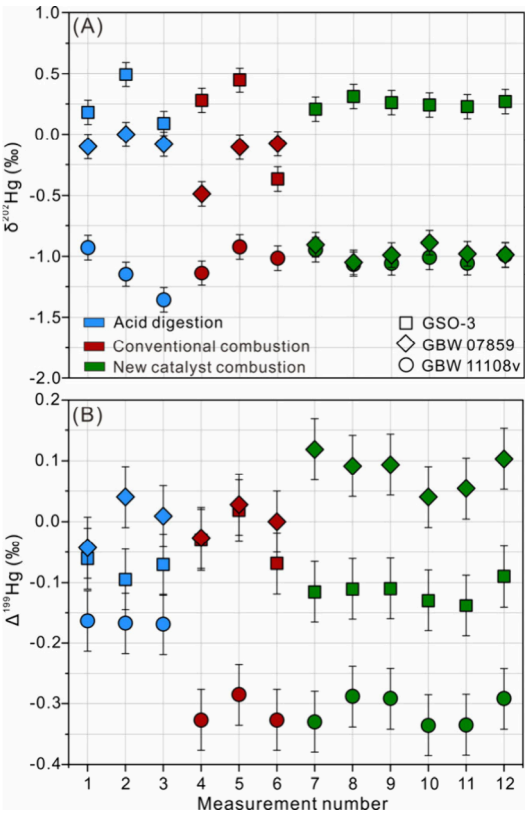

Figure 3. Plots of (A) δ^{202}Hg and (B) Δ^{199}Hg values for GBW 11108v, GSO-3 and GBW 07859 prepared using acid digestion, conventional combustion and new catalyst combustion.

elements (e.g., V, Cr, Co, Ni, Mo, Th, U, Ba, and REE), moderately volatile elements (e.g., Mn, Cu, Ag, Sb and As) and highly volatile elements (e.g., Zn, Tl, Pb, Cd, and Te).[24] The use of the catalyst-containing furnace quartz tube may greatly reduce the amount of interfering elements in the sample solutions. Analyses of trace elements in sample solutions prepared by the three pretreatment methods support our hypothesis (Supplementary Tables S4 and S5), as discussed below.

As shown in Figure 4. the digested solutions of the three SRMs display the highest contents of refractory elements, whereas their contents decreased by 2 to 4 orders of magnitude in solutions prepared by the dual-stage tube furnace system employing the traditional and the catalyst quartz tubes. The digested solutions of SRMs also contain high levels of moderately volatile elements, whereas their concentrations decreased by 2 to 6 orders of magnitude in solutions yielded from the dual-stage tube furnace system with both traditional and catalyst quartz tubes. The digested solutions of the SRMs display high levels of some highly volatile elements (Zn, Tl, Pb, and Cd), whereas their concentrations decreased by 2 to 5 orders of magnitude in solutions yielded from the dual-stage tube furnace system with both traditional and catalyst quartz tubes. Notably, Te concentrations did not decrease much using the traditional quartz tube, whereas they decreased by 2 to 5 orders of magnitude using the catalyst quartz tube. Given the poor Hg concentration recoveries and bias isotope results as well as high Te levels in sample solutions yielded by the two traditional methods, we believe that Te is the major interfering component for Hg isotopic analysis.

https://doi.org/10.1021/acs.analchem.4c03041
Anal. Chem. 2024, 96, 17560−17566

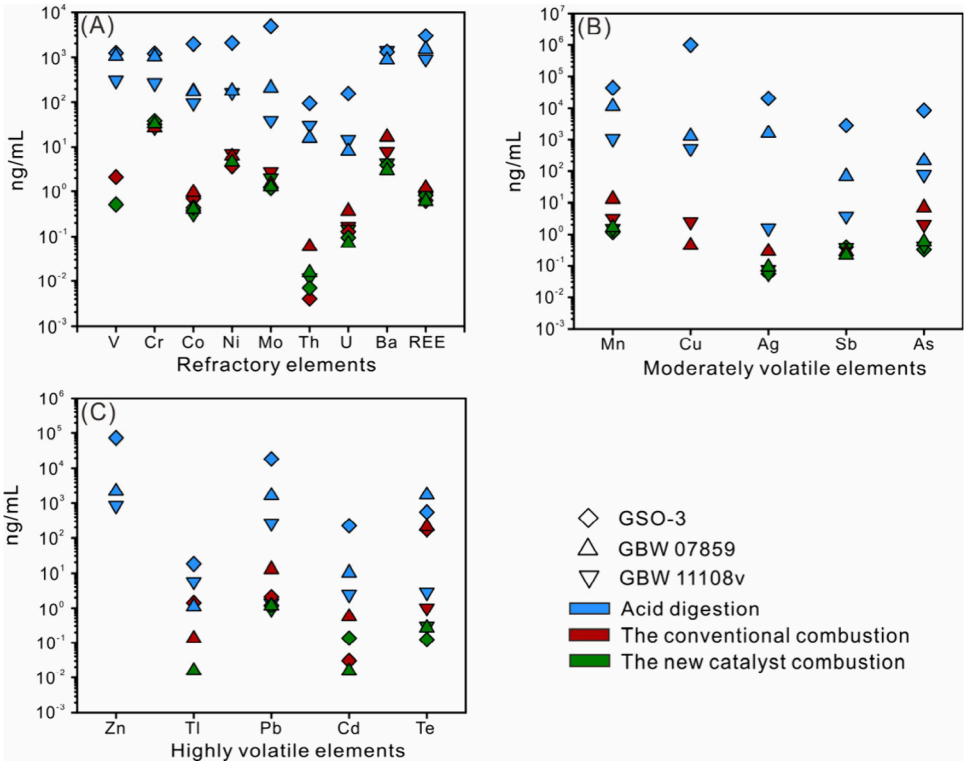

Figure 4. Plots of (A) refractory elements, (B) moderately volatile elements, and (C) highly volatile elements in GBW 11108v, GSO-3 and GBW 07859 prepared using acid digestion, conventional combustion and new catalyst combustion.

Sulfide minerals are enriched in Te due to the substitution of S by Te.[25,26] Since Te is a low melting point chalcophile element,[27] it can be released from sulfide ores during pretreatment by the dual-stage tube furnace. Te can also be dissolved in aqua regia during sample digestion. In trapping and digested solutions that display high acid concentrations (40%, v/v), Te occurs as soluble TeO_{2-3} or a TeO_{2-4} species. However, insoluble $HgTeO_3$ or $HgTeO_4$ species can form when acid concentrations decrease to low levels during the dilution of sample solutions to proper acid concentrations for Hg concentration and isotopic composition analyses. This would explain the low THg recoveries for sample solutions prepared by the two traditional methods, which contain Te levels of 2 to 6 magnitudes higher than those prepared by our new method (Table S5, Figure S1−S2). Although Te can also be released from the samples using our new method, our results suggest that the catalyst quartz tube can retain most of the released Te. The catalyst quartz tube contains 70% (w/w) of Mn dioxide, which is a strong oxidant and can react with Te to form nonmobile $MnTeO_3$ species in the catalyst quartz tube.[26,28]

Volcanic, magmatic and hydrothermal processes can lead to Te enrichment in geological samples.[26,29] Fumaroles, massive sulfides, and volcanogenic sulfur contain abundant Te.[26,30,31] Te rarely forms independent deposits apart from the Dashuigou and Majiagou deposits in China and the Kankberg deposit in Sweden.[26,32] Instead, Te typically occurs in magmatic and hydrothermal sulfide deposits.[32,33] Black shales, coals and red beds are also rich in Te.[34−36] Weathering of Te-bearing rocks could cause Te enrichment in soil and sediments.[37−39] Seawater contains low Te concentrations due to scavenging the main Te(IV) and Te(VI) species by Fe−Mn oxide/hydroxide particles.[40,41] Thus, Fe−Mn−Co crusts and nodules contain high Te levels.[32,42] Given that Te is widespread in geological and environmental samples, our new method opens up the possibility of understanding their Hg isotopic compositions.

Hg Isotopic Variation in Magmatic and Hydrothermal Sulfide Deposits. Magmatic and hydrothermal processes generate economically important sulfide deposits rich in Te.[26,43] The Hg isotopic composition of these deposits is yet poorly known due to a lack of methods for measuring Hg isotopes in Te-rich sulfides. Here, our new method was employed to measure the Hg isotopic composition of sulfide ore samples from the Jinchuan magmatic Ni−Cu sulfide deposit,[19] the Pulang porphyry Cu−Au deposit,[20] the Zhibula skarn Cu polymetallic deposit[21] in China. The results are listed in Supplementary Table S3 and Figure 5. Their Hg concentrations, based on analyses by the DMA-80 Hg analyzer, are 3.54 to 124 ppb for magmatic Ni−Cu sulfide ore samples and 57.0 to 609 ppb for porphyry sulfides. The Hg recoveries of our new method, based on the analysis of Hg concentration in the sample solutions, range from 92 to 103% (Figure 2).

Our new method yielded δ^{202}Hg values of −2.49 to −0.63‰ and Δ^{199}Hg values of −0.05 to 0.22‰ in magmatic Ni−Cu sulfide ore samples from the giant Jinchuan Ni−Cu sulfide deposit. Sulfides from the giant Pulang porphyry Cu−Au deposit[20] and the Zhibula skarn Cu polymetallic deposit[21] display δ^{202}Hg values of 0.06 to 0.6‰ and Δ^{199}Hg values of −0.19 to −0.07‰. Photoreduction of Hg(II) results in positive and negative Δ^{199}Hg values in Hg(II) and Hg(0) species, respectively.[2] Marine reservoirs (seawater and sediments) receive Hg mainly via atmospheric Hg(II) deposition and display positive Δ^{199}Hg values. However, terrestrial reservoirs (soil and vegetation) display negative Δ^{199}Hg values due to receiving Hg predominantly via atmospheric Hg(0)

https://doi.org/10.1021/acs.analchem.4c03041
Anal. Chem. 2024, 96, 17560−17566

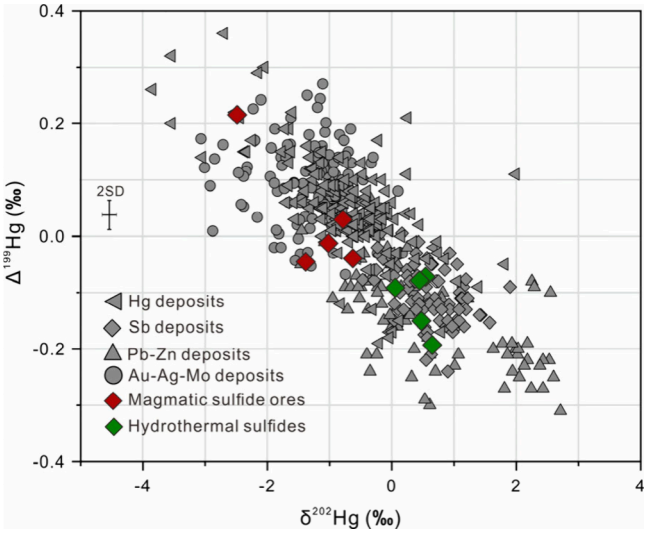

Figure 5. Hg isotopic composition of ore samples from magmatic sulfide deposits and hydrothermal sulfide deposits, in comparison to previous results on hydrothermal Pb−Zn deposits,[13,52] Au−Ag−Sb−Mo deposits,[23,50,53] Sb deposits[51,54] and Hg deposits.[36,37]

deposition.[3] The primitive mantle display near-zero Δ^{199}Hg values (0 ± 0.1‰, 2SD).[44] The upper continental crust shows near-zero Δ^{199}Hg values (0.03 ± 0.15‰).[45] As sedimentary, metamorphic, magmatic and hydrothermal processes do not produce Hg-MIF,[44−47] Δ^{199}Hg values can be a metallogenetic tracer.[48] The parent magma of the Jinchuan deposit was derived from the subcontinental lithospheric mantle (SCLM) modified by crustal marine materials,[19] which can explain the near-zero to positive Δ^{199}Hg values in the Jinchuan samples. The negative Δ^{199}Hg values of Pulang and Zhibula deposits developed at continental collisional settings confirm the previous hypothesis that hydrothermal fluids were mainly derived from recycled terrestrial materials,[49−51] due to terrestrial materials having negative Δ^{199}Hg values (−0.40 to 0.00 ‰).[3] The new results yielded from this study thus imply distinct Hg isotopic signatures in ore deposits formed in different geological settings, which is key to revealing their metallogeny, in particular, the source of metals.

CONCLUSIONS

We developed a dual-stage furnace system employing a catalyst tube to prepare sulfide samples for Hg isotope analysis. This new method can gain high Hg recovery, low concentrations of interfering elements, and accurate Hg isotopic ratios for sulfide samples and will aid in the use of Hg isotopes as a metallogenic tracer regarding the genesis of magmatic or hydrothermal sulfide deposits. This study demonstrates that Te can cause biased Hg isotopic ratios during Hg isotopic analysis, and special attention must be paid to preparing high-Te samples for Hg isotopic analysis.

ASSOCIATED CONTENT

Supporting Information

The Supporting Information is available free of charge at https://pubs.acs.org/doi/10.1021/acs.analchem.4c03041.

Supplementary Tables S1−S5 and Figures S1−S2 (PDF)

AUTHOR INFORMATION

Corresponding Author

Runsheng Yin − *State Key Laboratory of Ore Deposit Geochemistry, Institute of Geochemistry, Chinese Academy of Sciences, Guiyang 550081, China;* orcid.org/0000-0002-8072-0774; Email: yinrunsheng@mail.gyig.ac.cn

Authors

Lingjian Gao − *State Key Laboratory of Ore Deposit Geochemistry, Institute of Geochemistry, Chinese Academy of Sciences, Guiyang 550081, China; College of Earth Sciences, Jilin University, Changchun 130061, China*

Deyou Sun − *College of Earth Sciences, Jilin University, Changchun 130061, China*

Xueyun Wang − *State Key Laboratory of Ore Deposit Geochemistry, Institute of Geochemistry, Chinese Academy of Sciences, Guiyang 550081, China; University of Chinese Academy of Sciences, Beijing 100049, China*

Di Chen − *State Key Laboratory of Ore Deposit Geochemistry, Institute of Geochemistry, Chinese Academy of Sciences, Guiyang 550081, China; University of Chinese Academy of Sciences, Beijing 100049, China*

Zhendong Tian − *State Key Laboratory of Ore Deposit Geochemistry, Institute of Geochemistry, Chinese Academy of Sciences, Guiyang 550081, China*

Anbo Luo − *State Key Laboratory of Ore Deposit Geochemistry, Institute of Geochemistry, Chinese Academy of Sciences, Guiyang 550081, China*

Complete contact information is available at: https://pubs.acs.org/10.1021/acs.analchem.4c03041

Notes

The authors declare no competing financial interest.

ACKNOWLEDGMENTS

This research was funded by the Chinese Academy of Sciences through the Hundred Talent Plan.

REFERENCES

(1) Selin, N. E. *Annu. Rev. Env Resour* **2009**, *34*, 43−63.
(2) Bergquist, B. A.; Blum, J. D. *Science* **2007**, *318*, 417−420.
(3) Blum, J. D.; Sherman, L. S.; Johnson, M. W. *Annu. Rev. Earth Planet Sci.* **2014**, *42*, 249−269.
(4) Yang, L.; Yu, B.; Han, D.; Zhang, K.; Liu, H.; Xiao, C.; Hu, L.; Yin, Y.; Shi, J.; Jiang, G. *Critical Reviews in Environmental Science and Technology* **2023**, *53*, 1935−1956.
(5) Wang, X.; Yuan, W.; Lin, C. J.; Feng, X. *Critical Reviews in Environmental Science and Technology* **2022**, *52*, 3763−3786.
(6) Foucher, D.; Hintelmann, H. *Anal. Bioanal. Chem.* **2006**, *384*, 1470−1478.
(7) Yin, R. S.; Feng, X. B.; Foucher, D.; Shi, W. F.; Zhao, Z. Q.; Wang, J. *Chinese Journal of Analytical Chemistry* **2010**, *38*, 929−934.
(8) Yin, R. S.; Krabbenhoft, D. P.; Bergquist, B. A.; Zheng, W.; Lepak, R. F.; Hurley, J. P. *J. Anal At Spectrom* **2016**, *31*, 2060−2068.
(9) Geng, H.; Yin, R.; Li, X. *J. Anal At Spectrom* **2018**, *33*, 1932−1940.
(10) Yin, R.; Feng, X.; Li, X.; Yu, B.; Du, B. *Trends in Environmental Analytical Chemistry* **2014**, *2*, 1−10.
(11) Meng, M.; Sun, R. Y.; Liu, H. W.; Yu, B.; Yin, Y. G.; Hu, L. G.; Shi, J. B.; Jiang, G. B. *Environ. Sci. Technol.* **2019**, *53*, 2460−2471.
(12) Yin, R. S.; Deng, C. Z.; Lehmann, B.; Sun, G. Y.; Lepak, R. F.; Hurley, J. P.; Zhao, C. H.; Xu, G. W.; Tan, Q. P.; Xie, Z. J.; et al. *Acs Earth Space Chem.* **2019**, *3*, 1631−1639.

(13) Xu, C. X.; Yin, R. S.; Peng, J. T.; Hurley, J. P.; Lepak, R. F.; Gao, J. F.; Feng, X. B.; Hu, R. Z.; Bi, X. W. *Miner Deposita* **2018**, *53*, 339−352.
(14) Yin, H.; Yao, H.; Yuan, W.; Lin, C. J.; Fu, X.; Yin, R.; Meng, B.; Luo, J.; Feng, X. *Anal. Chem.* **2023**, *95*, 12290−12297.
(15) Biswas, A.; Blum, J. D.; Bergquist, B. A.; Keeler, G. J.; Xie, Z. Q. *Environ. Sci. Technol.* **2008**, *42*, 8303−8309.
(16) Sun, R.; Enrico, M.; Heimburger, L. E.; Scott, C.; Sonke, J. E. *Anal Bioanal Chem.* **2013**, *405*, 6771−6781.
(17) Wang, X.; Luo, J.; Yin, R.; Yuan, W.; Lin, C. J.; Sommar, J.; Feng, X.; Wang, H.; Lin, C. *Environ. Sci. Technol.* **2017**, *51*, 801−809.
(18) Zerkle, A. L.; Yin, R. S.; Chen, C. Y.; Li, X. D.; Izon, G. J.; Grasby, S. E. *Nat. Commun.* **2020**, *11*, 1709.
(19) Gao, L. J.; Long, T. M.; Sun, D. Y.; Deng, C. Z.; Tian, Z. D.; Song, X. Y.; Yin, R. S. *Geochem Geophy Geosy* **2022**, *23*, No. e2022GC010349.
(20) Cao, K.; Yang, Z. M.; White, N. C.; Hou, Z. Q. *Econ Geol* **2022**, *117*, 57−90.
(21) Wang, S.; Cao, M.; Li, G.; Evans, N. J.; Silang, W.; Qin, K. *Ore Geol Rev.* **2023**, *160*, 105601−105615.
(22) Lopez-Anton, M. A.; Yuan, Y.; Perry, R.; Maroto-Valer, M. M. *Fuel* **2010**, *89*, 629−634.
(23) Deng, C.; Sun, G.; Rong, Y.; Sun, R.; Sun, D.; Lehmann, B.; Yin, R. *Geology* **2021**, *49*, 309−313.
(24) McDonough, W. F.; Sun, S.-s. *Chem. Geol.* **1995**, *120*, 223−253.
(25) Simon, G.; Essene, E. J. *Econ Geol* **1996**, *91*, 1183−1208.
(26) Missen, O. P.; Ram, R.; Mills, S. J.; Etschmann, B.; Reith, F.; Shuster, J.; Smith, D. J.; Brugger, J. *Earth-Sci. Rev.* **2020**, *204*, 103150−103179.
(27) Frost, B. R.; Mavrogenes, J. A.; Tomkins, A. G. *Can. Mineral.* **2002**, *40*, 1−18.
(28) Grundler, P. V.; Brugger, J.; Etschmann, B. E.; Helm, L.; Liu, W.; Spry, P. G.; Tian, Y.; Testemale, D.; Pring, A. *Geochim. Cosmochim. Acta* **2013**, *120*, 298−325.
(29) Brugger, J.; Liu, W.; Etschmann, B.; Mei, Y.; Sherman, D. M.; Testemale, D. *Chem. Geol.* **2016**, *447*, 219−253.
(30) Yu, M. Z.; Chen, X. G.; Garbe-Schönberg, D.; Ye, Y.; Chen, C. T. A. *Minerals* **2019**, *9*, 245−263.
(31) Okrugin, V.; Favero, M.; Liu, A.; Etschmann, B.; Plutachina, E.; Mills, S.; Tomkins, A. G.; Lukasheva, M.; Kozlov, V.; Moskaleva, S.; et al. *Am. Mineral.* **2017**, *102*, 1736−1746.
(32) Fu, Y.; Huang, S.; Li, J.; Zhang, J. *Bulletin of Mineralogy, Petrology and Geochemistry* **2023**, *42*, 741−754.
(33) Guo, X.; Zhou, T.; Fan, Y. *Acta Petrologica Sinica* **2023**, *39*, 3139−3155.
(34) Belzile, N.; Chen, Y. W. *Appl. Geochem.* **2015**, *63*, 83−92.
(35) Parnell, J.; Spinks, S.; Brolly, C. *Precambrian Res.* **2018**, *305*, 145−150.
(36) Parnell, J.; Spinks, S.; Bellis, D. *Terra Nova* **2016**, *28*, 221−227.
(37) Hayes, S. M.; Ramos, N. A. *Environmental Chemistry* **2019**, *16*, 251−265.
(38) Bullock, L. A.; Perez, M.; Armstrong, J. G.; Parnell, J.; Still, J.; Feldmann, J. *Ore Geol Rev.* **2018**, *99*, 411−424.
(39) Qin, H. B.; Takeichi, Y.; Nitani, H.; Terada, Y.; Takahashi, Y. *Environ. Sci. Technol.* **2017**, *51*, 6027−6035.
(40) Harada, T.; Takahashi, Y. *Geochim. Cosmochim. Acta* **2008**, *72*, 1281−1294.
(41) Hein, J. R.; Koschinsky, A.; Halliday, A. N. *Geochim. Cosmochim. Acta* **2003**, *67*, 1117−1127.
(42) Fu, Y.; Wen, H. *Ore Geol Rev.* **2020**, *121*, No. 103470.
(43) Keith, M.; Smith, D. J.; Jenkin, G. R. T.; Holwell, D. A.; Dye, M. D. *Ore Geol Rev.* **2018**, *96*, 269−282.
(44) Moynier, F.; Jackson, M. G.; Zhang, K.; Cai, H. M.; Halldorsson, S. A.; Pik, R.; Day, J. M. D.; Chen, J. B. *Geophys. Res. Lett.* **2021**, *48*, No. e2021GL094301.
(45) Tian, Z.; Lehmann, B.; Deng, C.; Luo, A.; Zhang, X.; Moynier, F.; Yin, R. *Geochim. Cosmochim. Acta* **2023**, *361*, 200−209.
(46) Yin, R.; Chen, D.; Pan, X.; Deng, C.; Chen, L.; Song, X.; Yu, S.; Zhu, C.; Wei, X.; Xu, Y.; et al. *Nat. Commun.* **2022**, *13*, 948.
(47) Chen, D.; Ren, D.; Deng, C.; Tian, Z.; Yin, R. *Geochim. Cosmochim. Acta* **2022**, *334*, 231−240.
(48) Yin, R.; Wang, X.; Sun, R.; Gao, L.; Deng, C.; Tian, Z.; Luo, A.; Lehmann, B. *Chem. Geol.* **2024**, *654*, 122063−122074.
(49) Wang, Q.; Liu, X.; Yin, R.; Weng, W.; Zhao, H.; Yang, L.; Zhai, D.; Li, D.; Ma, Y.; Groves, D. I. *Geology* **2024**, *52*, 115−119.
(50) Deng, C.; Lehmann, B.; Xiao, T.; Tan, Q.; Chen, D.; Tian, Z.; Wang, X.; Sun, G.; Yin, R. *Earth Planet Sci. Lett.* **2022**, *593*, 117646−117653.
(51) Fu, S. L.; Hu, R. Z.; Yin, R. S.; Yan, J.; Mi, X. F.; Song, Z. C.; Sullivan, N. A. *Miner Deposita* **2020**, *55*, 1353−1364.
(52) Liu, Y. F.; Qi, H. W.; Bi, X. W.; Hu, R. Z.; Qi, L. K.; Yin, R. S.; Tang, Y. Y. *Chem. Geol.* **2021**, *559*, 119910−119923.
(53) Gao, L.; Sun, D.; Tian, Z.; Luo, A.; Lehmann, B.; Yin, R. *Chem. Geol.* **2024**, *645*, 121880−121889.
(54) Deng, C.; Zhang, J.; Hu, R.; Luo, K.; Zhu, Y.; Yin, R. *Science China Earth Sciences* **2022**, *65*, 269−281.

https://doi.org/10.1021/acs.analchem.4c03041
Anal. Chem. 2024, 96, 17560−17566